



SPE 56822

Geostatistical Scaling Laws Applied to Core and Log Data

P. Frykman, SPE, Geological Survey of Denmark and Greenland (GEUS), and C.V. Deutsch, SPE, University of Alberta

Copyright 1999, Society of Petroleum Engineers Inc.

This paper was prepared for presentation at the 1999 SPE Annual Technical Conference and Exhibition held in Houston, Texas, 3-6 October 1999.

This paper was selected for presentation by an SPE Program Committee following review of information contained in an abstract submitted by the author(s). Contents of the paper, as presented, have not been reviewed by the Society of Petroleum Engineers and are subject to correction by the author(s). The material, as presented, does not necessarily reflect any position of the Society of Petroleum Engineers, its officers, or members. Papers presented at SPE meetings are subject to publication review by Editorial Committees of the Society of Petroleum Engineers. Electronic reproduction, distribution, or storage of any part of this paper for commercial purposes without the written consent of the Society of Petroleum Engineers is prohibited. Permission to reproduce in print is restricted to an abstract of not more than 300 words; illustrations may not be copied. The abstract must contain conspicuous acknowledgment of where and by whom the paper was presented. Write Librarian, SPE, P.O. Box 833836, Richardson, TX 75083-3836, U.S.A., fax 01-972-952-9435.

Abstract

Reconciling data from different scales is a longstanding problem in reservoir characterization. Data from core plugs, well logs of different types, and seismic data must all be accounted for in the construction of a geostatistical reservoir model. These data are at vastly different scales and it is inappropriate to ignore the scale difference when constructing a geostatistical model.

Geostatistical scaling laws were devised in the 1960s and 1970s primarily in the mining industry where the concern was mineral grades in selective mining unit (SMU) blocks of different sizes. These principles can be extended to address problems of core, log and seismic data. The adoption of these classic volume-variance or scaling relationships presents some challenges. Some specific concerns are (1) the ill-defined volume of measurement, (2) uncertainty in the small-scale variogram structure, and (3) non-linear averaging of many responses including acoustic properties and permeability.

We demonstrate the application of volume-variance relations for upscaling and downscaling techniques to integrate data of different scales. Practical concerns are addressed with data from a chalk reservoir in the Danish North Sea. A direct sequential simulation algorithm accounting for data at all scales is documented.

Introduction

Within the petroleum industry and many other fields where geostatistical models are constructed, the treatment of data of different scale is often ignored¹. The core and log data may be averaged in the vertical direction to the scale of the modelling cells²; however, this only partially addresses scale difference. In other examples, a fine-scale model is constructed and then numerically averaged to larger scale³⁻⁵. This may be applied in

a nested fashion due to computational limitations. The direct simulation of gridblock values conditioned to fine-scale data carried out by cosimulation using cross-covariance between fine- and coarse-scale values has been described⁶.

Notwithstanding the importance of accounting for data at different scales, the use of geostatistical scaling laws has not seen wide application in petroleum geostatistics. This is due mainly to unfamiliarity with the techniques and scaling laws. Recalling and demonstrating such techniques will address this unfamiliarity.

The scaling laws tell us how the variogram changes with volumetric scale⁷. As scale increases, the range of correlation increases, the variance and variogram sill decrease, and the nugget effect also decreases.

After a recall of theory, the application of scaling laws is illustrated with a synthetic example and with real data from a Danish chalk reservoir. Core and well log data are used. These data measure significantly different volumes. The volume of the core measurement is well understood; however, the volume of the interpreted well log derived porosity is less well understood. The statistics of each data type together with analytical volume-variance relationships can be used to quantify the volume of investigation of the well log data. An illustration of the different scales (Fig. 1) shows that the change of scale from core to log measurement volumes is nearly as large as the jump from log volume to that of a geological modelling cell.

The ultimate goal of this work is to illustrate how data of different scales may be used simultaneously in the construction of high-resolution geostatistical models. When the different types of data are all "hard," in the sense that they do not contain significant errors or uncertainties relative to the property being modeled, it is possible to use block kriging. Certain data types such as seismic contain uncertainties related to the great distance of measurement and calibration of the measured acoustic properties to the petrophysical properties of interest. In this case, it is necessary to use block cokriging.

Recall of Volume-Variance Scaling Relationships

*Mining Geostatistics*⁸ is the classic reference for volume-variance scaling relationships. The essential results are recalled below. Details and proofs may be found in the original reference.

Consider the fitted variogram model at arbitrary scale v , where v often represents the small core scale:

$$\gamma_v(\mathbf{h}) = C_v^0 + \sum_{i=1}^{nst} C_v^i \cdot \Gamma^i(\mathbf{h}) \quad (1)$$

where $\gamma_v(\mathbf{h})$ is the variogram model at the v scale, C_v^0 is the nugget effect, nst is the number of nested variogram structures used to fit the variogram, C_v^i is the variance contribution of each nested structure, $i=1, \dots, nst$, and $\Gamma^i(\mathbf{h})$ are the nested structures consisting of an analytical function (spherical, exponential, Gaussian, hole-effect, etc.) and six anisotropy parameters (three angles and three distance ranges). Note that the ‘‘sill’’ of the analytical nested structure Γ is unity; the C coefficients describe the variance contribution of each structure. The sum of the variance contributions is the variance at the v -scale also known as the dispersion variance

$$D^2(v, A) = C_v^0 + \sum_{i=1}^{nst} C_v^i \quad (2)$$

where $D^2(v, A)$ is the variance of volumes of size v in the entire area of interest A . The mean value at a larger (or smaller) scale does not change, assuming arithmetic average. The variance, however, decreases as the volume increases; high and low values are averaged out as the volume of investigation or measurement increases. As the variance decreases the variogram structure also changes. The variance contributions C_v^i , $i=0, \dots, nst$, decrease. The shape of each nested structure $\Gamma^i(\mathbf{h})$ may also change.

Experience has shown that the variogram shape change is small. The three correlation ranges increase as the averaging volume increases; however, the actual ‘‘shape’’ of the variogram changes very little. The range at a larger volume V increases as the increase in volume size ($|V|/|v|$) in each particular direction:

$$a_v = a_p + (|V| - |v|) \quad (3)$$

Depending on the shape of the larger volume V , the range may increase in some directions and stay the same in other directions. Assuming the variogram shape does not change, we have to quantify how the variance contributions C_v^i , $i=0, \dots, nst$, change.

It can be shown that the purely random component, represented by the nugget effect, decreases with an inverse relationship of the volume, i.e.,

$$C_V^0 = C_v^0 \cdot \frac{|v|}{|V|} \quad (4)$$

In this case $|v|$ and $|V|$ represent the volume of each scale, respectively.

Average variogram or ‘‘gamma-bar’’ values are used to determine how the variance contribution of each nested structure decreases:

$$C_V^i = C_v^i \cdot \frac{1 - \bar{\Gamma}(V, V, \mathbf{a}^i)}{1 - \bar{\Gamma}(v, v, \mathbf{a}^i)} \quad (5)$$

The ‘‘gamma-bar’’ notation represents the average variogram for vectors where each end of the vector independently describes the volume V or v . In 3D the gammabar values may be expressed as the infamous sextuple integrals of early geostatistics. The modern approach, however, is to calculate all gamma-bar values numerically. For the present investigation the calculation of the gammabar values is performed with a program using a cylindrical shaped volume. This has been found the most realistic volume geometry in the case of working with well data from cores and logs. For other shapes of the scaling volumes, a version with box shaped volume is available.

Scaling Relations with synthetic example

In order to show the application of the scaling rules for data obtained at different scales, we have generated a synthetic fine-scale 1-D model. The program SASIM⁹ based on simulated annealing has been used to simulate the model using the input of a target histogram and a variogram with a spherical variogram model. The scale of the 1-D modeling cell has been chosen to be 0.02 m in order to mimic the fine scale geological information normally available from core plugs. The resulting model is illustrated in Fig. 2. The block average values for each non-overlapping 0.5 m segment are calculated from the fine scale data. The resulting averaged data is shown in Fig.2.

The histograms at the two different scales are shown in Figs. 3 and 4. The variance is reduced significantly from 3.57 to 1.99 due to the averaging. The variogram model used for simulating the synthetic case is a spherical model with 0.54 m range and zero nugget. The sill value of 3.6 is supplied by the target histogram. The simulation is seen to reproduce nicely the variogram model (Fig. 5).

Derivation of Point-Scale Variogram

The scaling laws developed above may be applied on each nested structure in the variogram. As the first step the point scale variogram must be deduced. The scaling laws are concerned with the changes to the nugget effect, the variogram range and the sill. For the downscaling to point-scale from our data, we need to consider all three elements.

The fine-scale data has no nugget effect in the correlation structure. Therefore the point-scale variogram is assumed to have no nugget.

For the spherical structure the correction to point variogram range a_p based on the fine-scale range a_v is: $a_p = a_v - (|v| - |p|)$, see equation (3) above. Where p = point scale, which is zero and v = fine-scale, which is 0.02 m. Thus, the

corrected range for the spherical nested structure is $= 0.54 - (0.02 - 0) = 0.52$ m

The sill of each basic structure is corrected according to equation (5) presented above. The `gammabar` program is used to calculate the needed $\bar{\Gamma}(v, v)$ values. The mean variogram value at the point scale is, of course, zero. For all calculations of mean variogram values we assume one dimensional averaging of the data.

The value for $\bar{\Gamma}(v, v)$ for the spherical structure can be calculated with the `gammabar` program, using the point-scale variogram description as unit variogram between 0 and 1 with range 0.52 m as derived above. For calculation of $\bar{\Gamma}(v, v)$, the volume v is defined as the fine scale dimension of 2 cm, giving a $\bar{\Gamma}(v, v)_{\text{sph}}$ value of 0.021, and a resulting point-scale sill C_p of 3.65 for the spherical structure, as compared to the fine-scale sill value of the spherical structure of 3.57.

In summary the point-scale variogram structure is therefore defined as having zero nugget and a spherical structure with range 0.52 m and sill of 3.57.

Application of Scaling Laws for Prediction of Coarse-Scale Variogram from Fine-Scale Variogram

The theoretically derived variogram for coarse-scale may be calculated and compared to the experimental variogram from the block-averaged coarse-scale data. The closeness of the match is a measure of the efficacy of the scaling relations described above.

As stated above on equation (3), the range of the coarse-scale variogram range a_v may be calculated based on the fine-scale range a_v , that is, $a_v = a_v + (|V| - |v|)$. Where v is the fine-scale of dimension 0.02 m and V is the coarse-scale at 0.50 m resolution. This results in a range correction for the variogram from the fine-scale to coarse-scale as follows:

$$a_v = 0.54 + (0.50 - 0.02) = 1.02 \text{ m}$$

The sill of each basic structure in the variogram model is modified as in equation (5). The required $\bar{\Gamma}(v, v)$ (0.02 m) and $\bar{\Gamma}(V, V)$ (0.5 m) values can be calculated with the `gammabar` program, using as input the point-scale variogram which has been derived earlier from the core data. For the structure, $\bar{\Gamma}(v, v) = 0.0213$ and $\bar{\Gamma}(V, V) = 0.434$. The variance for the fine-scale data for the structure $C_v = 2.82$, and we therefore derive the log-scale sill for the structure $C_v = 2.82 * (1 - 0.434 / 1 - 0.0213) = 2.06$. The comparison of the theoretically predicted coarse-scale variogram and the experimental variogram obtained from the block averaged data is shown in Fig. 5, having a very good agreement.

In order to further outline the performance of the scaling laws, the procedure has been applied at other coarse scale

resolutions of 1.0, 2.0 and 4.0 m block averages. The comparison between the theoretical predictions and the experimental variograms gives a near perfect match as is shown in Fig. 6.

In order to illustrate the evolution of the variogram, the decrease in sill (variance) is shown as a function of the averaging volume in Fig. 7. However, this function is only valid for this particular model construction, and heavily depends on the variogram structure at the fine scale level.

The synthetic fine-scale model has also been used to investigate how non-overlapping volume averaging influences the upscaling of variograms. For this purpose a moving 0.5 m window filter has been applied with a simple square filter function on the fine scale data. The resulting experimental variogram shows that the variogram structure is changing from the original fine scale spherical model into a more Gaussian shaped model for the moving average data as seen in Fig. 8.

Scaling Relations with Real Data

Data from an interval in the MFB-7 well from the Dan Field in the Danish North Sea will be considered. The Dan Field is an Upper Maastrichtian to Lower Paleogene chalk limestone reservoir, and is characterised by high porosities (30-40 %) and generally low permeabilities (1 mD)¹⁰. From the wellbore has been extracted a section of data covering approximately 18 m of vertical section, see Fig. 9. Since the well is deviated approximately 32 degrees, any length measures derived from the original wellbore have to be adjusted by a factor 0.84 ($= \cos 32^\circ$). This affects the calculation of the scaling factors and the averaging volume of the logging tool, and we have chosen to work in the space of TVD (True Vertical Depth). This decision is based on having a good horizontal continuity in the layered formation drilled, and therefore the variability within the deviated well bore is the same as in the projected vertical section, see Fig. 10.

The section shows cyclic porosity variations probably caused by climatic variations during deposition of the pelagic chalk material¹¹. The core measurements represent a volume of about 5x2x2 cm (vertical resolution 0.02 m). The log measurements represent an average over approximately 0.60 m (2 ft.) of the well-bore (corresponding to a 0.50 m vertical section in this particular example), and with an uncertain investigation depth probably around 0.25 m.

As expected, the core plug porosity values show greater variability than the log porosity values. The histograms shown in Figs. 11 and 12 illustrate the difference.

The core and well log porosity values are both considered excellent measurements with little measurement or interpretation error. Figure 13 shows a cross plot of the core versus log porosity values. The scatter on this plot is attributable both to the different measurement volumes, as well as to the different physics behind the measurements. The cross plot of core and log porosity shows a fair correlation between the two variables. The comparison shows that the well log data does not represent some of the high porosity layers recorded by the core analysis samples.

The core-porosity semivariogram shows clear cyclic variations with a period at about 1.90 m (Fig. 14). The variogram model has no nugget effect and two nested structures: (1) a spherical structure with sill equal to 2.82 and range of 0.54 m, and (2) a hole effect model with amplitude 1.2 and peak at 0.95 m. The fit of this nested model is quite good. Figs. 15 and 16 show the two elementary nested structures to be considered in the scaling relationships.

Derivation of Point-Scale Variogram

The scaling laws developed previously are applied on each nested structure in the variogram.

The core-scale data shows no nugget effect. Detailed investigations at the millimeter-scale also shows no nugget.

For the spherical structure the correction to point variogram range a_p based on the core-scale range a_v is: $a_p = a_v - (|v| - |p|)$, see equation (3) above. Where p = point scale, which is zero and v = plug scale, which is 0.02 m. Thus, the corrected range for the spherical nested structure is $= 0.54 - (0.02 - 0) = 0.52$ m

For the hole effect structure, the wavelength for the periodic structure is not affected, and the peak distance used for the modelling is kept constant at 0.95 m for the point scale variogram.

The sill of each basic structure is corrected according to equation (5) presented above. The `gammabar` program is used to calculate all needed $\bar{\Gamma}(v, v)$ values. For all calculations of mean variogram values we assume only one dimensional averaging of the data. This entails that our well data are only averaged in the vertical direction, which is a fair assumption given that we have a layered formation with large horizontal continuity. Therefore, the investigation depth is not to be considered in this case.

The value for $\bar{\Gamma}(v, v)$ for the spherical structure can be calculated with the `gammabar` program, using the point-scale variogram description. For calculation of $\bar{\Gamma}(v, v)$, the volume v is defined as the core-plug volume of 5x2x2 cm with a vertical length scale measure of 2 cm, giving a $\bar{\Gamma}(v, v)_{sph}$ value of 0.021, and a resulting point-scale sill C_p of 2.88 for the spherical structure, as compared to the core-scale sill value of the spherical structure of 2.82.

The same procedure is used for the hole effect variogram for the amplitude scaling, giving $\bar{\Gamma}(v, v)_{hole} = 0.0005$, and therefore a virtually unchanged variance contribution of 1.2 for the point scale variogram.

In summary, the point-scale variogram structure has zero nugget and two nested structures: (1) a spherical structure with range 0.52 m and sill of 2.88, and (2) a hole effect structure with peak at 0.95 and a variance contribution of 1.2.

Application of Scaling Laws to obtain variance at coarse-scale

The point (\bullet) variance within an arbitrary volume v is equal to the mean value $\bar{\gamma}$ of $\gamma(h)$ for all h and all directions within that volume, where $\gamma(h)$ is the point-scale variogram consisting of all nested structures, that is,

$$\sigma^2(\bullet, v) = \bar{\gamma}(v, v) \quad (6)$$

furthermore, given a larger region R , the additivity of variance entails that,

$$\sigma^2(\bullet, R) = \sigma^2(\bullet, v) + \sigma^2(v, R) \quad (7)$$

for any volume v . In words, the variance of points \bullet in a region R is equal to the variance of points within a larger volume v plus the variance of that larger volume v within the region R .

Let's consider two different volumes v and V (e.g. core and log scale volumes). $\sigma^2(\bullet, R)$ is the global stationary point scale variance. Applying relation (7) to volumes v and V , the experimental average variogram $\bar{\gamma}(V, V)$ for the log-scale volume may be expressed as:

$$\bar{\gamma}(V, V) = \bar{\gamma}(v, v) + \sigma^2(v, R) - \sigma^2(V, R) \quad (8)$$

In our case:

$$\bar{\gamma}(V, V) = \bar{\gamma}(v, v) + 4.02 - 2.23$$

Now $\bar{\gamma}(v, v)$ can be calculated with the `gammabar` program given the real point scale variograms as defined earlier, and as the sum of the contribution from the two structures in the nested model, we obtain the experimental $\bar{\gamma}(V, V)$ as:

$$\begin{aligned} \bar{\gamma}(V, V) &= \bar{\gamma}(v, v) + 4.02 - 2.23 \\ &= \bar{\gamma}(v, v)_{sph} + \bar{\gamma}(v, v)_{hole} + 4.02 - 2.23 \\ &= 0.061 + 0.0006 + 4.02 - 2.23 = 1.85 \end{aligned}$$

Which then gives us an independent assessment of the average variogram value within log-scale volumes.

Conversely, if uncertainty exists about the averaging volume, the volume variance scaling laws may also be applied to check the volume V for the coarse-scale data collected, now that we have an independent $\bar{\gamma}(V, V)$ value.

Assessment of Tool Investigation Volume

Given the small-scale core data variogram and the experimental log-scale variogram we can determine the volume of measurement of the well-log. This volume is determined in an iterative fashion until the `gammabar` prediction of variance matches the actual well log-derived variance.

Provided we have established a reliable estimate of the point-scale variogram it is possible to calculate the theoretical $\bar{\gamma}(V, V)$ for a range of different volume scales. Then, the actual volume scale can be determined where the theoretical $\bar{\gamma}(V, V)$ matches the experimental $\bar{\gamma}(V, V)$.

Applying this procedure with the point-scale variogram model derived above leads to the results in Fig. 17. The cross plot shows that the experimental value for $\bar{\gamma}(V, V)$ of 1.85 matches the theoretical values at a scale of 0.62 m.

This volume of 0.62 m is the measure of the vertical averaging, and has to be calculated back to the tool measurement geometry in the inclined wellbore. This gives an effective tool resolution of 0.74 m, which is somewhat close to the 0.60 m that is predicted from the physics of the logging tool, which is a LDT (Litho-Density-Tool). The tool resolution is reported to be 0.30 m (= 12 inches); the measurements are recorded at every 0.15 m, and the effective resolution in the logged data is therefore usually considered to be around 0.60 cm due to the tool movement. The discrepancy between the two tool resolution estimates (0.74 vs. 0.60 m) is explained by the lack of the additional variance that would exist in the true density data that forms the basis for the log interpretation. This variance in the density data would exist at the tool resolution volume, and will show up on a cross plot of measured bulk density and measured porosities for a given formation. However, for the practical log-interpretation a regression is performed and the log-interpreted porosity is developed via an equation maybe incorporating some lithology correction and noise reduction effects. Therefore the derived log porosity is a smoothed version of the true porosity distribution even if it was quantified over the tool volume scale average, and this smoothing causes us to believe that the tool is larger than the actual physical tool. The smoothing effect is also seen relating back to Fig. 9 where deviation between the core and log values is seen in some locations.

This illustrates that the comparison of different data types therefore also involves cross-scaling in addition to up- or down-scaling as it has been outlined by Corbett et al.¹². The cross-scaling is the determination of a relationship between two different physical properties, whereas up-scaling is the determination of an effective (or pseudo) property at a scale larger than that of the original measurement. The definition of these terms is a help to separate the impact of geology (largely up-scaling) from that of the physics (largely cross-scaling) in a more systematic manner¹².

The moving average effect for the density logging tool used causes the averaged values captured with the tool to be derived from overlapping volumes, which might not fully satisfy the basic assumption behind the scaling rules that is valid only for non-overlapping volumes. This might have consequences also for the shape of the variograms for the different data types. The experimental variogram for moving average values tends to behave like it has an underlying gaussian model, even if the original fine-scale data is honouring a spherical model. In practise it means that in cases

where the log data is modelled with a gaussian variogram model, the derived point-scale variogram for scaling purposes, or any variograms at smaller scales, could be considered to have a spherical model.

Prediction of Log-Scale Variogram from the Core-Scale Variogram

The theoretically derived variogram for log-scale may be calculated and compared to the experimental variogram from log-scale data. The closeness of the match is a measure of the efficacy of the scaling relations described above.

As stated above in equation (3), the range of the log-scale variogram range a_V may be calculated based on the core-scale range a_v . That is, $a_V = a_v + (|V|/|v|)$, where v is the core-scale of dimension 0.02 m and V is the coarse-scale at 0.50 m resolution. In this context we refer to the tool resolution of 0.60 m converted into 0.50 m the TVD space. This results in a range correction for the spherical structure from the core-scale to log-scale as follows:

$$a_V sph = 0.54 + (0.50 - 0.02) = 1.02 \text{ m}$$

For the hole effect structure the peak distance is not changed from the original 0.95 m.

The sill of each basic structure in the variogram model is modified as in equation (5). The required $\bar{\Gamma}(v, v)$ (0.02 m) and $\bar{\Gamma}(V, V)$ (0.5 m) values can be calculated with the gammabar program, using as input the point-scale variogram which has been derived earlier from the core data. For the spherical structure, $\bar{\Gamma}(v, v) sph = 0.0213$ and $\bar{\Gamma}(V, V) sph = 0.434$. The variance for the core data for the spherical structure $C_v sph = 2.82$, and we therefore derive the log-scale sill for the spherical structure $C_V sph = 2.82 * (1 - 0.434 / 1 - 0.0213) = 1.63$.

Likewise for the hole effect structure, $\bar{\Gamma}(v, v) hole = 0.00049$ and $\bar{\Gamma}(V, V) hole = 0.207$. The variance contribution for the core data hole effect $C_v hole = 1.2$, and we therefore get the log scale sill for the hole effect structure: $C_V hole = 1.2 * (1 - 0.29 / 1 - 0.00036) = 0.97$.

The total sill value for the log scale data is predicted as the sum of these two contributions of 1.63 and 0.97 = 2.60, which compares not quite with the actual sill of 2.23 found in the actual log porosity data set. As explained earlier, the theoretically derived variance is higher than the measured variance because of the error or additional variance that is filtered out during the conversion from measured bulk density in the formation via the wireline-log interpretation routine. The difference amounts to 14 % in this case, which we think can easily be explained by the missing error in the density measures.

The theoretical variogram model derived for the log-scale is compared to the experimental data from the log-scale data, see Fig. 18. In order to illustrate the effect of the cross-scaling

uncertainty, the figure is showing both the theoretical prediction of the variogram based on 0.50 m vertical averaging corresponding to the normally accepted 0.60 m effective tool resolution, and a second variogram is based on the estimated vertical averaging volume of 0.62 m (= 0.74 m tool resolution).

Simulation accounting for multiple scales

Rigorous data integration calls for simultaneously using data from different scales in the construction of a numerical model. This section presents a program, `dssim_ms`, for direct sequential simulation (DSS) with multiscale data.

This program performs DSS with multiscale data assuming linear averaging. Each input data value is “tagged” by a shape factor and a volume. The shape factor species a rectangular parallelepiped or a cylindrical volume. The volume is specified by three length scales oriented with the principal X,Y,Z grid or by a radius in the X-Y plane and a length scale in the Z direction. An arbitrary number of different data-scales may be used to create realizations at another, different, volume-scale. The histogram at the volume scale being simulated must be specified. In practice, this is derived from the data using an affine or indirect lognormal volume-variance correction. The use of direct simulation versus Gaussian simulation calls for no a-priori data transformation. There is, however, an implicit multiGaussian random function model due to the averaging (kriging) of random numbers (simulated values). Although any number of data scales may be used, it is anticipated that the primary use of the program will be to use core and log data to directly estimate the geological modeling cells, see Fig. 19 for a schematic illustration. Larger scale data from seismic or historical production may also be used in modeling. All data is assumed to be “hard”, that is, with no measurement errors. The only difference between the different data is the volume scale.

Simple kriging with a stationary known mean is used. Ordinary kriging or kriging with a trend model could be implemented; however, the unbiasedness constraint(s) would have to account for the volume scale of the data. The simple kriging estimator for two different data scales is written:

$$z^* - \bar{z} = \sum_{i=1}^n \lambda_{vi} \cdot [z_v(\mathbf{u}_i) - \bar{z}] + \sum_{i=1}^m \lambda_{Vi} \cdot [z_V(\mathbf{u}_i') - \bar{z}] \quad (9)$$

where z^* is the estimator, \bar{z} is the mean, there are n data at scale v , $z_v(\mathbf{u}_i)$, $i=1, \dots, n$, and m data at scale V , $z_V(\mathbf{u}_i')$, $i=1, \dots, m$. The set of $n+m$ kriging weights λ_{vi} , $i=1, \dots, n$, λ_{Vi} , $i=1, \dots, m$ are given by the classical simple kriging equations. The equations are presented graphically in Fig. 19. Some notes on the construction and use of this matrix:

The diagonal elements, $C(v_i, v_i)$, $i=1, \dots, n$ and $C(V_i, V_i)$, $i=1, \dots, m$ on the left hand side matrix are covariances between the data and themselves, that is, the dispersion variance of the data volumes within the study area $D^2(v, A)$ and $D^2(V, A)$.

The dispersion variances for all data scales are calculated by average variogram $\bar{\gamma}$ values.

The covariances between the data of different volumes, all non-diagonal elements on the left-hand side, are calculated by numerical averaging the point covariance structures. The covariances between the data and the volume being estimated, the right-hand side vector, are calculated by numerical averaging of the point covariance structures.

Solution of the kriging equations leads to the optimal weights to calculate the estimator (see equation 9) and the kriging variance:

$$\sigma_K^2 = D^2(B, A) - \sum_{i=1}^n \lambda_{vi} \cdot C(v_i, B) - \sum_{i=1}^m \lambda_{Vi} \cdot C(V_i, B) \quad (10)$$

DSS proceeds sequentially by drawing from a distribution with mean and variance specified by the kriging mean and variance. The shape of the distribution is not specified. Any distributional shape may be used and the input variogram/covariance structure will be reproduced. The histogram of the simulated values, however, will not honor the input histogram. Each simulated realization may be transformed with `trans` to honor the target histogram.

The present program `dssim_ms` considers each distribution to have a normal or Gaussian shape. This is consistent with application to porosity where the histograms are often symmetric with a near-normal shape. Any other distribution could be used. A lognormal distribution would be more appropriate for permeability.

The shape of the resulting histogram will not be correct due to the implicit assumptions of the DSS approach. The `trans` program from GSLIB may be used to get back to the correct histogram.

The variogram specification in `dssim_ms` corresponds to the point scale. The nugget effect is not defined at the point scale, therefore, there is one additional parameter to specify which scale the nugget corresponds to. Note that it is not possible to simulated true point values (zero volume) in presence of a nugget effect.

Simulation example

For illustrating the procedure of multiscale direct simulation we establish a data set including data at three different scales, core, log and seismic scale. The core and log data originates from the section already used for the variogram analysis in the chapter on scaling laws. In addition a synthetic data set with seismically derived porosity values is included with a resolution of 4 m. The point scale variogram derived earlier is used for specifying the correlation structure, and a first simulation is created at a resolution of 0.02 m, comparable to the core scale resolution. A comparison of the simulated values and the data is shown in Fig. 20.

Discussion

The theoretical upscaling applied on one example seems to match very well the actual data despite some uncertainties regarding the size of the log-scale averaging volume. In fact,

the back-calculation of the averaging volume from the spatial statistics could prove a useful supplement to analytical calculations regarding well log tool response.

The upscaling example matches despite a periodic structure in the data, and this has given rise to an extension of the traditional scaling rules with a separate rule for periodic components in the variogram description.

Conclusions and Future Work

The increasing diversity of data available for use in geostatistical modeling, and the urge to incorporate them all into the modelling procedures have raised the issue of scaling of the different data.

The traditional scaling laws have been revived and made available for numerical analysis.

A simulation algorithm that is able to account for data at multiple scales has been implemented and the output compared to data input.

There remain, however, some significant assumptions with that must be addressed in future work.

A significant assumption is that the petrophysical property must average linearly. This is appropriate for facies indicator variables and porosity; however, acoustic properties and permeability simply do not average linearly. A power-law formalism could be used whereby the original variable is transformed to a variable that, in general, averages linearly. The widely used sequential simulation approaches require a transformation either at the beginning to the convenient Gaussian distribution or afterwards to correct for the non-reproduction of the histogram. Such transforms are not compatible with the assumptions behind the classical volume-variance relations of geostatistics.

Another significant assumption in the use of conventional volume-variance relations is that the spatial variability is completely characterized by a stationary random function using 2-point variogram / covariance measures of correlation. No higher order non-linear spatial connectivity is accounted for, which may pose a serious problem in real petroleum reservoirs.

Nomenclature

a	=	range parameter for variogram.
C	=	sill parameter for variogram.
C_v^0	=	nugget value for variogram.
D^2	=	variance.
R	=	large scale region.
TVD	=	True vertical depth.
V	=	volume for coarse scale .
v	=	volume for fine scale.
\bullet	=	point scale.
$\Gamma^i(\mathbf{h})$	=	function describing the correlation structure for a model variogram.

γ	=	variance for variogram calculation.
$\bar{\gamma}$	=	average variogram for a defined volume.
$\bar{\Gamma}(V, V)$	=	average variogram using unit variogram from 0 to 1 for a defined volume.

Subscripts

$hole$	=	hole effect in variogram model.
sph	=	spherical structure for variogram model.

References

- Almeida, A.S. and Frykman, P.: "Geostatistical modelling of chalk reservoir properties in the Dan Field, Danish North Sea," *Stochastic Modeling and Geostatistics; Principles, Methods, and Case Studies*, J.M. Yarus and R.L. Chambers (eds.), American Association of Petroleum Geologists, Tulsa (1995) AAPG Computer Applications in Geology, **3**, 273-286.
- Cox, D.L., *et al.*: "Integrated modeling for optimum management of a giant gas condensate reservoir, Jurassic eolian Nugget Sandstone, Anschutz Ranch East Field, Utah Overthrust (U.S.A.)," *Stochastic Modeling and Geostatistics; Principles, Methods, and Case Studies*, J.M. Yarus and R.L. Chambers (eds.), American Association of Petroleum Geologists, Tulsa (1995) AAPG Computer Applications in Geology, **3**, 287-321.
- Damsleth, E. and Tjølsen, C.B.: "Scale consistency from cores to geologic description," *SPE Formation Evaluation* (1994) 295-299.
- Wen, X.H. and Gomez-Hernandez, J.: "Upscaling Hydraulic Conductivities in Cross-Bedded Formations," *Mathematical Geology* (1998) **30**, 2, 181-211.
- Sweet, M.L., Blewden, C.J., Carter, A.M. and Mills, C.A.: "Modeling heterogeneity in a low-permeability gas reservoir using geostatistical techniques, Hyde Field, Southern North Sea," *American Association of Petroleum Geologists Bulletin* (1996) **80**, 11, 1719-1735.
- Gomez-Hernandez, J.J. and Journel, A.G.: "Stochastic Characterization of Grid-Block Permeabilities," *SPE Formation Evaluation* (1994) 93-99.
- Kupfersberger, H., Deutsch, C.V., and Journel, A.G.: "Deriving constraints on small-scale variograms due to variograms of large-scale data," *Mathematical Geology* (1998) **30**, 7, 837-852.
- Journel, A.G., and Huijbregts, C.: *Mining geostatistics*, Academic Press, New York City (1978) 600.
- Deutsch, C.V. and Journel, A.G.: *GSLIB - Geostatistical Software Library and User's guide*, 2nd ed., Oxford University Press, New York City (1997) 340.
- Kristensen, L., *et al.*: "A multidisciplinary approach to reservoir subdivision of the Maastrichtian chalk in the Dan Field, Danish North Sea," *American Association of Petroleum Geologists Bulletin* (1995) **79**, 11, 1650-1660.
- Scholle, P.A., Albrechtsen, T., and Tirsgaard, H.: "Formation and diagenesis of bedding cycles in uppermost Cretaceous chalks of the Dan Field, Danish North Sea," *Sedimentology* (1998) **45**, 2, 223-243.
- Corbett, P.W.M., Jensen, J.L., and Sorbie, K.S.: "A review of up-scaling and cross-scaling issues in core and log data interpretation and prediction," *Core-Log Integration*, P.K. Harvey and M.A. Lovell (eds.), Geological Society, London (1998) Geological Society Special Publications, **136**, 9-16.

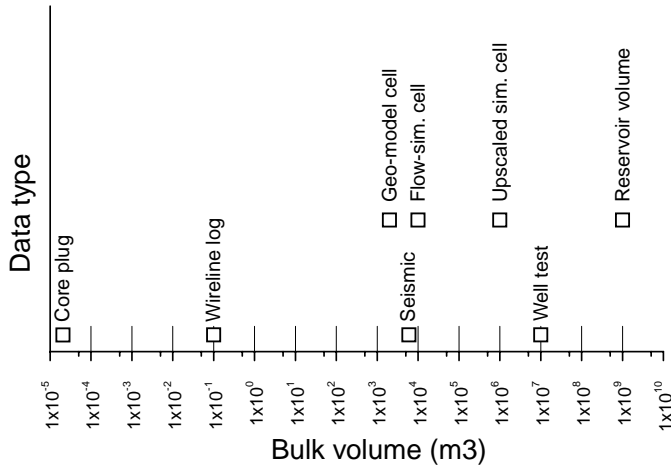


Fig. 1 – Illustration of the volume measures (in cubic metres) for the different scales of data. Note that the scale distance between core and wireline-log is nearly as large as between log- and modelling cell volumes.

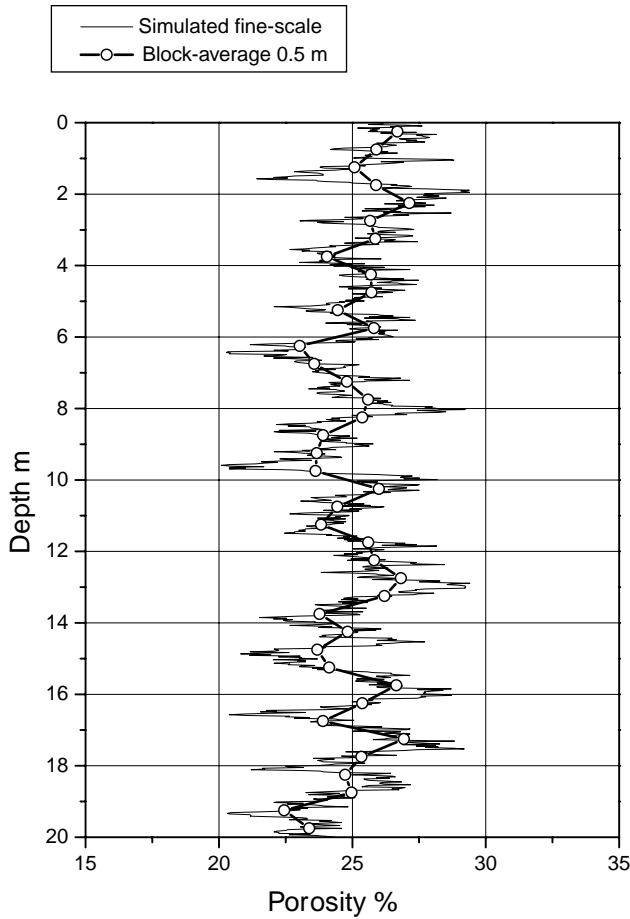


Fig. 2 - Profile of the simulated porosity data at 0.02 m scale (thin line), and the block averaged values for 0.50 m scale (dots and thick line).

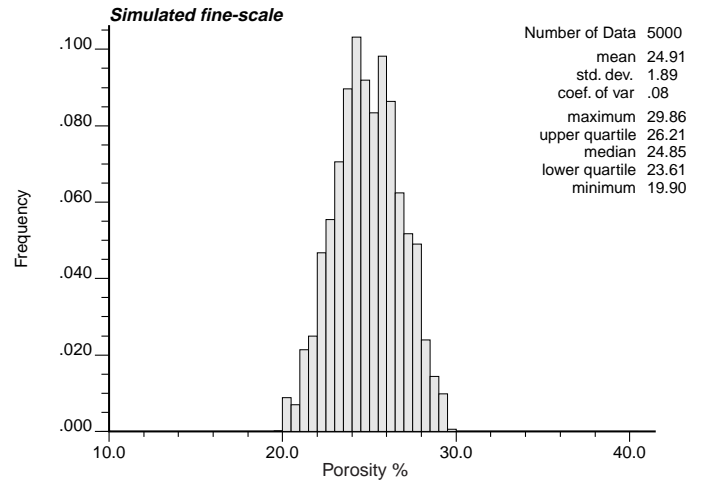


Fig. 3 – Histogram of simulated fine-scale porosity in the profile.

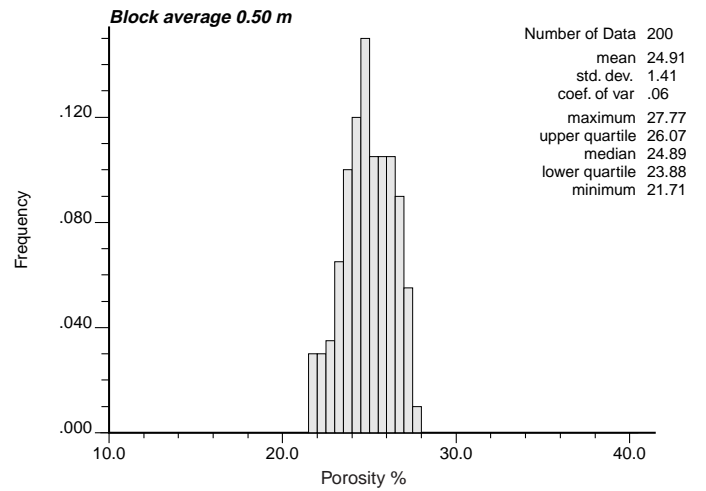


Fig. 4 - Histogram of porosity values after block-averaging over 0.50 m intervals of the fine-scale simulation.

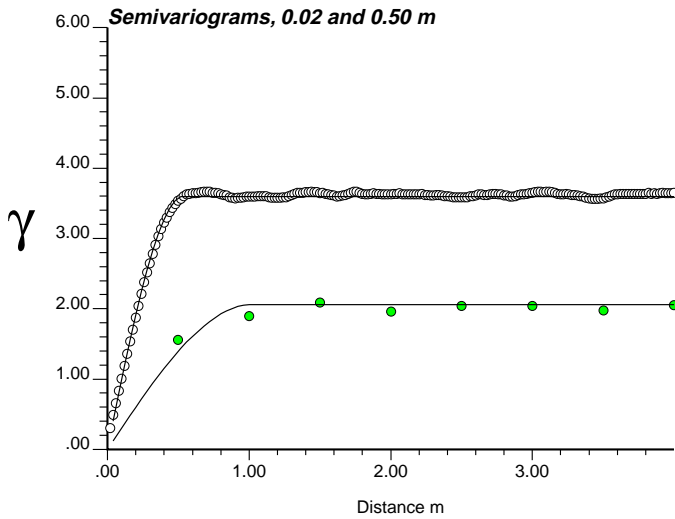


Fig. 5 – Variograms for fine-scale and blockaveraged porosity values. Upper set is model variogram (line) and experimental variogram (dots) of simulated fine-scale showing a very good reproduction by the simulation. The lower set is the theoretically predicted variogram (line) and the experimental variogram for the block-average porosity values (dots).

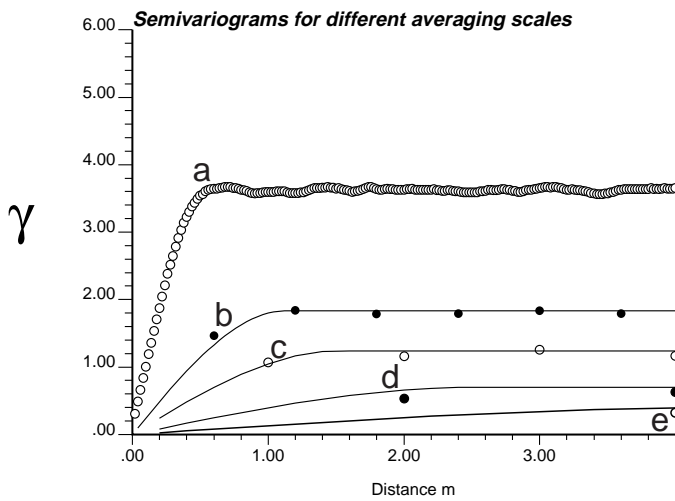


Fig. 6 – Comparison of theoretical and experimental variograms for a - fine-scale simulation; b - 0.50 m blockaverage; c - 1 m blockaverage; d - 2 m blockaverage; e - 4 m blockaverage. They all show very good match between prediction and experimental variogram.

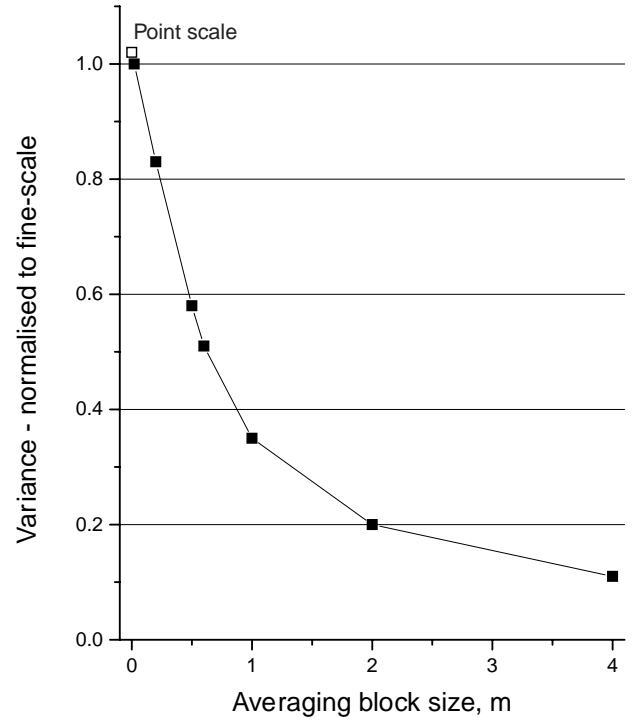


Fig. 7 - Illustration of the decrease in sill value (normalised to the sill for the 0.02 m data = core-scale) for the theoretically predicted variograms as the length scale of averaging is increased in steps from 0.20 m to 4.0 m

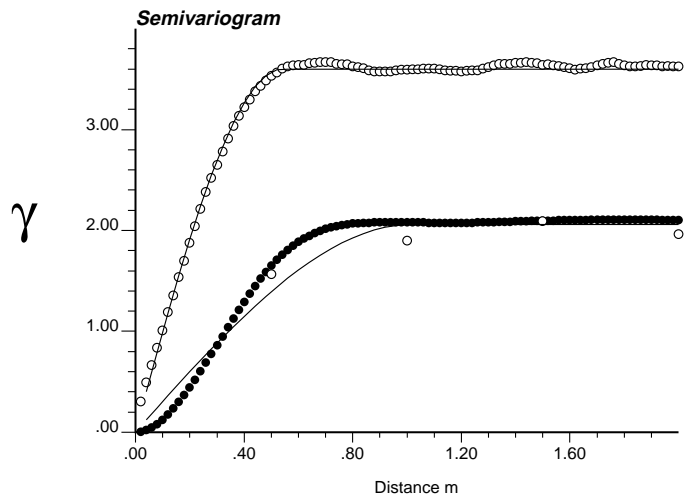


Fig. 8 – Model and experimental variograms of the original fine scale simulation (upper line and open dots) and the experimental variogram for the upscaled data using a moving window average (lower filled dots) indicating a more Gaussian type variogram model. The open dots is the experimental variogram for the block-averaged data. The lower line is the predicted variogram model assuming spherical structure in the scaling calculation.

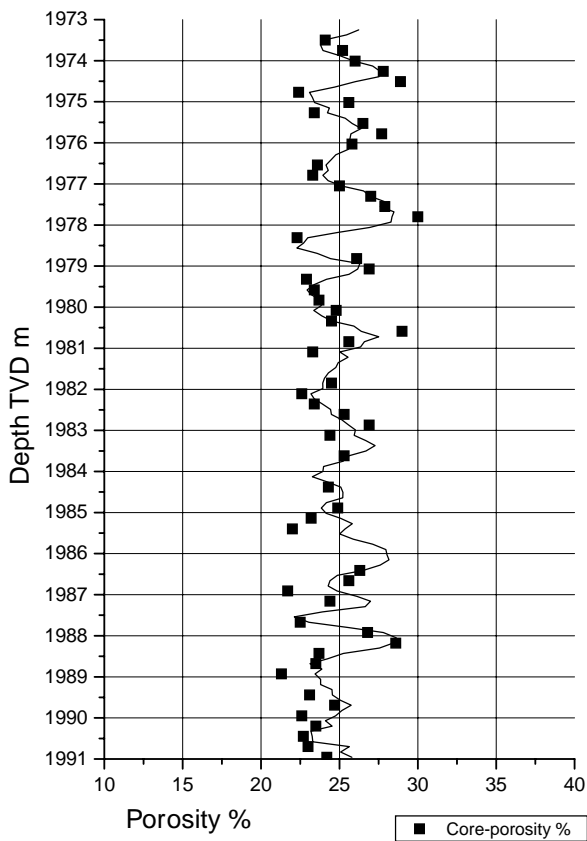


Fig. 9 - Profile of the core plug and porosity log data from the well MFB-7 in a 20 m interval. Note the general agreement of the core and log porosity data, and the greater variability in the core data. The periodic variations are clearly observed especially in the upper part.

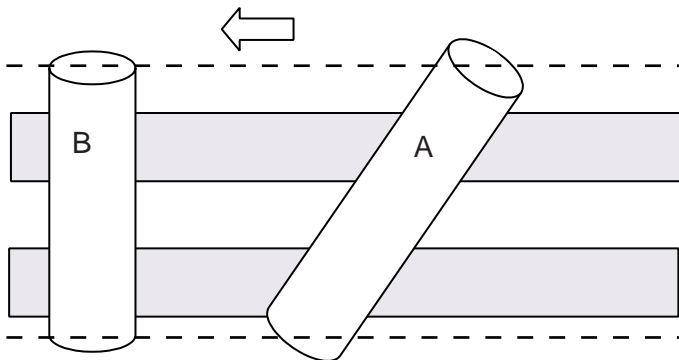


Fig. 10 - Schematic illustration of tool volume (length) conversion from measured depth scale to TVD (True Vertical Depth) scale.

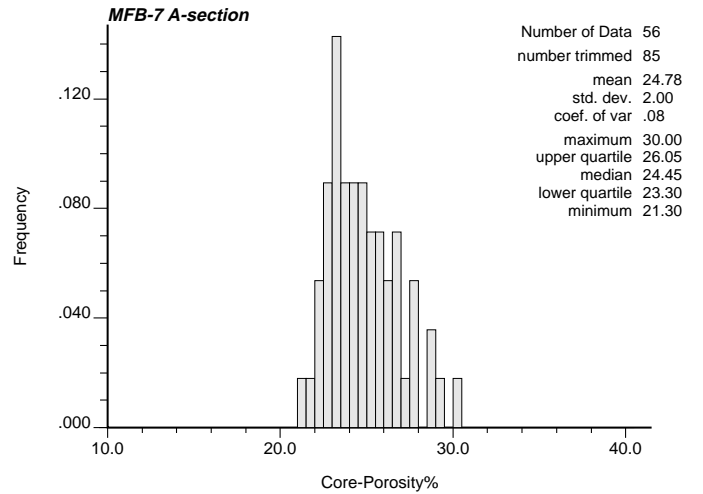


Fig. 11- Histogram of porosity core data from the MFB-7 interval.

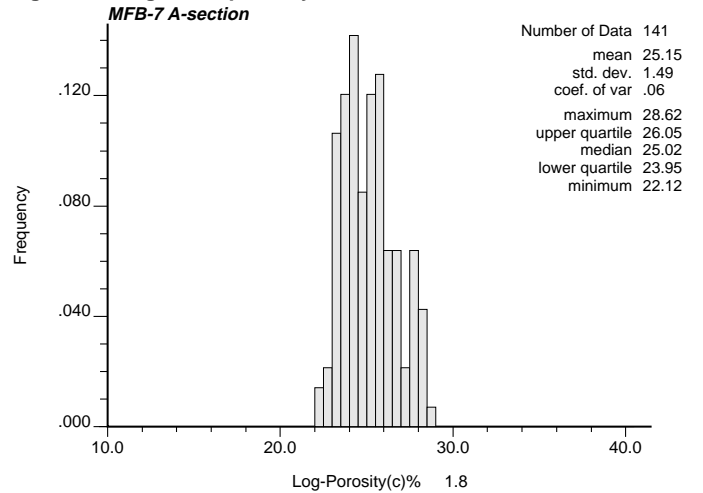


Fig. 12 - Histogram of porosity log data from the MFB-7 interval. Note that the log data has lesser variance than the core data in Fig. 10.

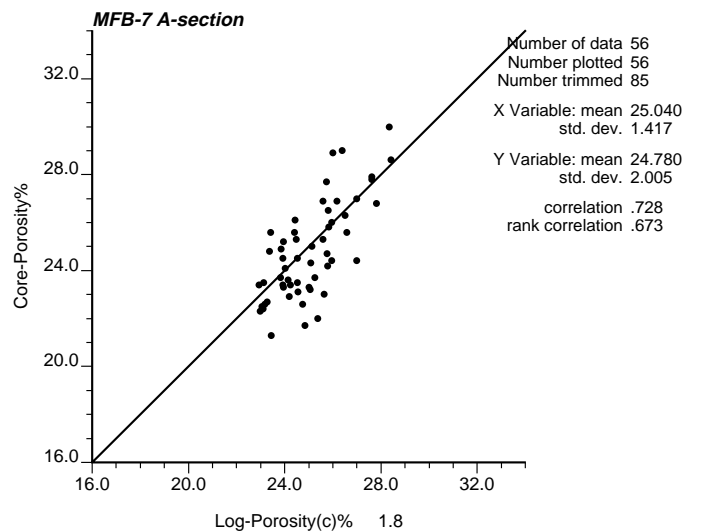


Fig. 13 - Cross plot of log and core porosity data from the MFB-7 interval. Note the fair correlation and the difference in variance.

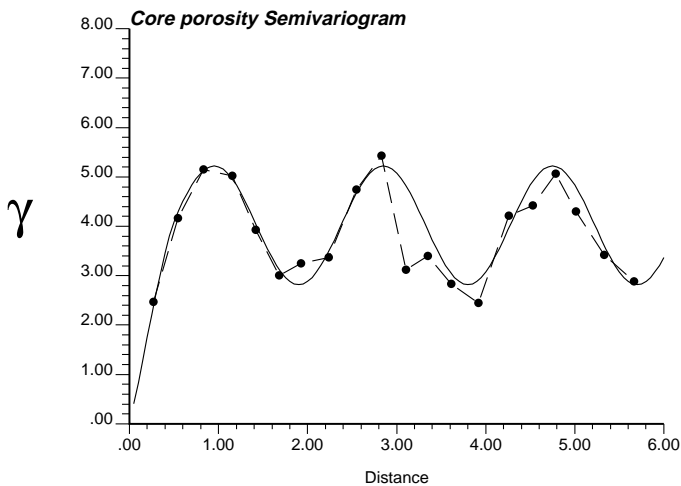


Fig. 14 - Experimental variogram of core porosity data from the MFB-7 interval. The experimental variogram has been fitted with a nested model of spherical and hole effect variogram models.

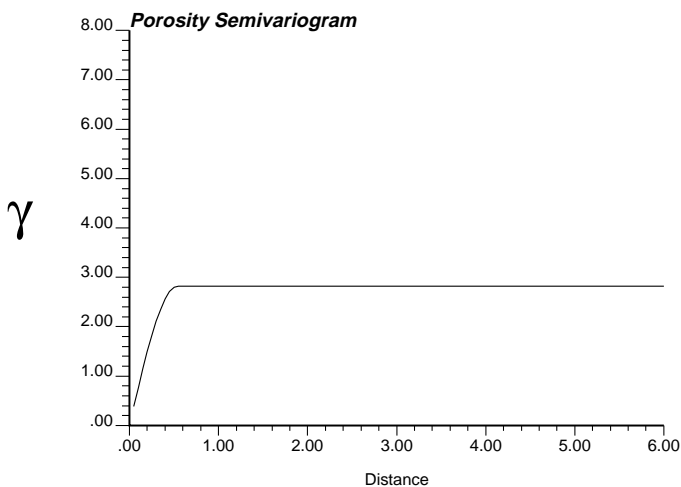


Fig. 15 - Individual variogram structure for the spherical component of the nested variogram structure in Fig. 14.

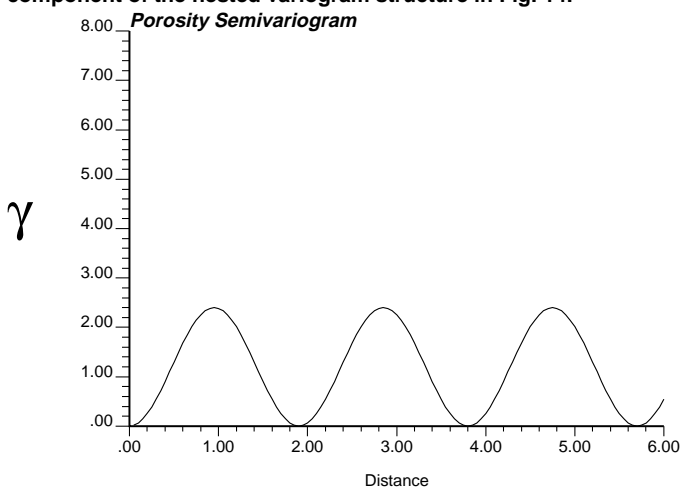


Fig. 16 - Individual variogram structure for the hole effect (periodic) component of the nested variogram structure in Fig. 14.

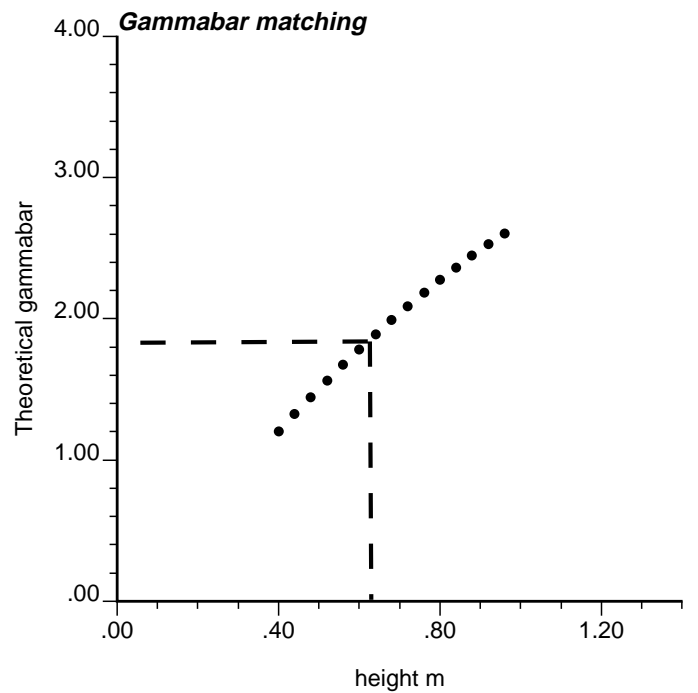


Fig. 17 - Cross plot of the theoretical average variogram $\bar{\gamma}(V, V)$ versus the volume V for length scales close to the tool investigation length. The average variogram value of 1.84 is known experimentally permitting an estimate of the scale of investigation, that is, 0.62m

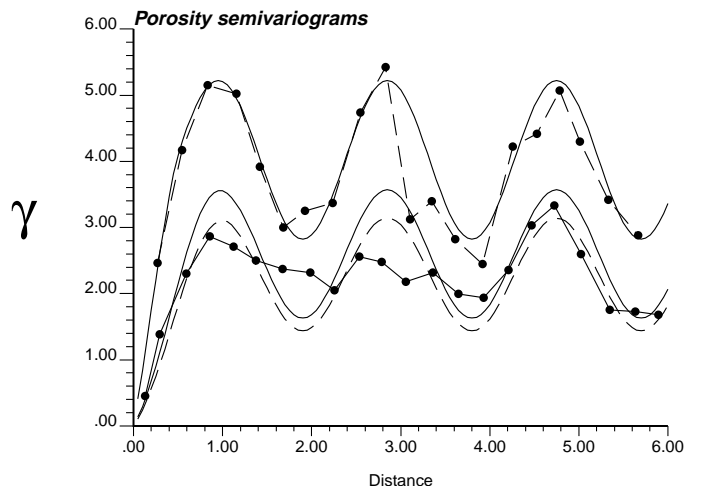


Fig. 18 - Comparison of core scale experimental variogram (upper bullets connected by dashed line), core scale variogram model (upper solid line), log-scale experimental variogram (lower bullets connected by line), theoretically derived log-scale variogram (lower solid line). The lower dashed line is the model calculated with using a slightly too large tool volume (0.6 m) which seems to match better the actual experimental variogram from the log scale data.

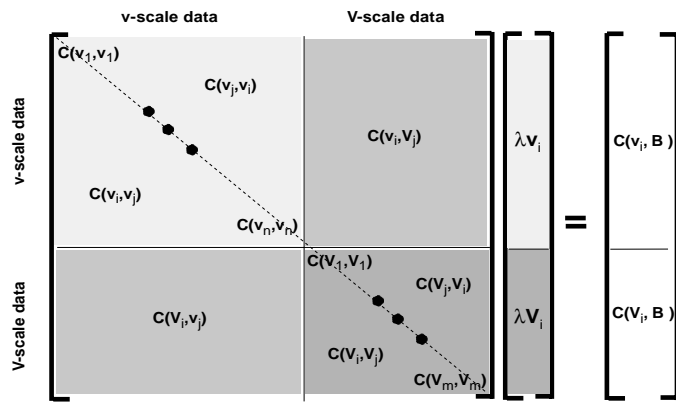


Fig. 19 – Illustration of the simple kriging matrix for multiscale data. v and V represent two different data scales, B represents the block scale being estimated.

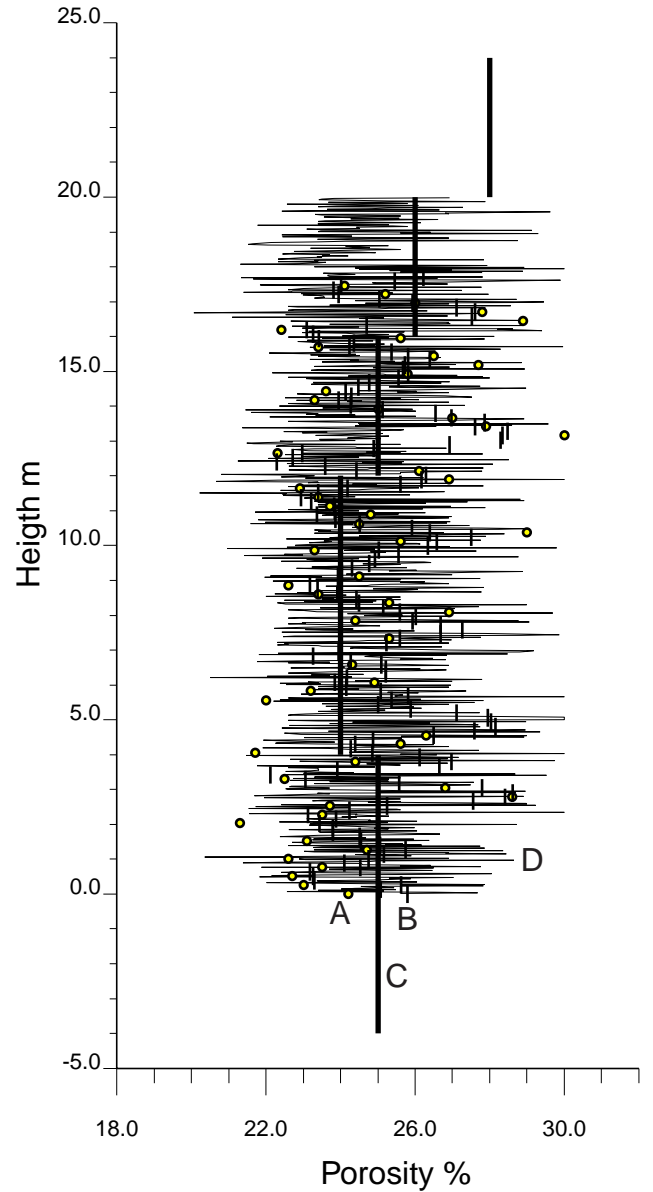


Fig. 20 – Illustration of the data at three different scales (dots A=core 0.02 m, short dashes B=log 0.50 m, long lines C=seismic 4.0 m) used for a direct multiscale simulation at 0.02 m scale shown as thin line (D).